Finite Range Interactions and the Constrained Molecular Dynamics

M.Papa INFN -CATANIA

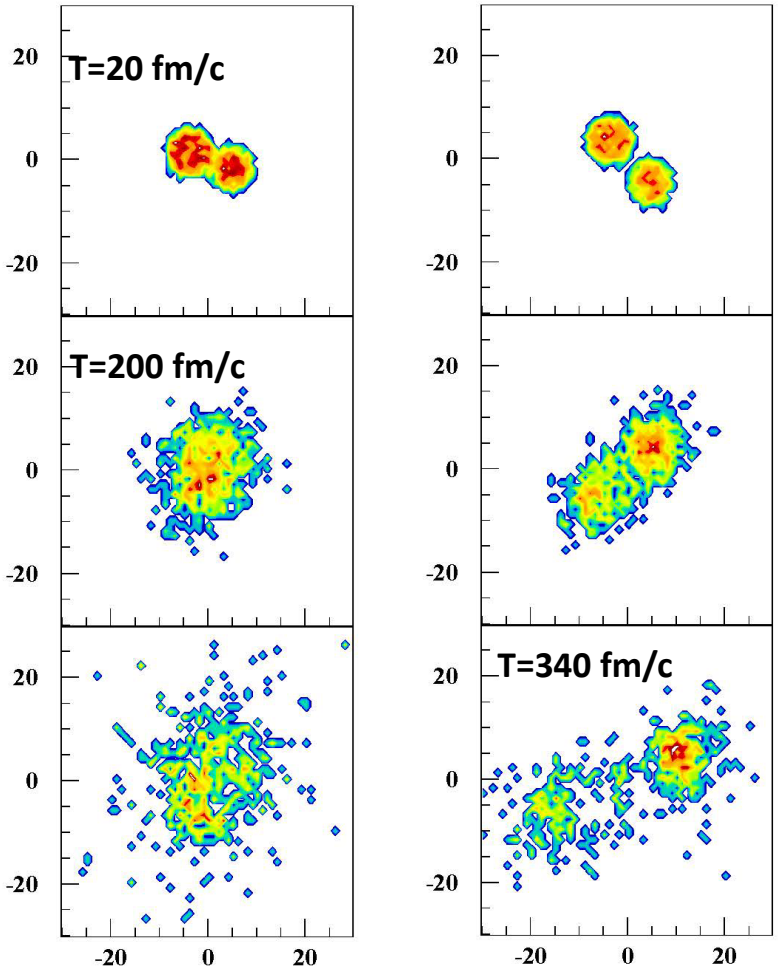

- Study of correlations included in the semi-classical molecular dynamics models (CoMD), and their influence on the energy density functionals. Comparison with the semiclassical Mean Field approach. The study is performed for NM in the case of finite range interactions.

- Study of the effects associated to the finite range interactions on reaction mechanisms induced on the system ^{64}Ni+^{48}Ca at different incident energies.

M. Papa, T. Maruyama, A. Bonasera, Phys. Rev. C 64 (2001) 024612

M. Papa, G. Giuliani, A. Bonasera, J. Comp. Phys. 208 (2005) 403,

M.Papa, Phys.Rev C 87 014001 (2013)

TMEP

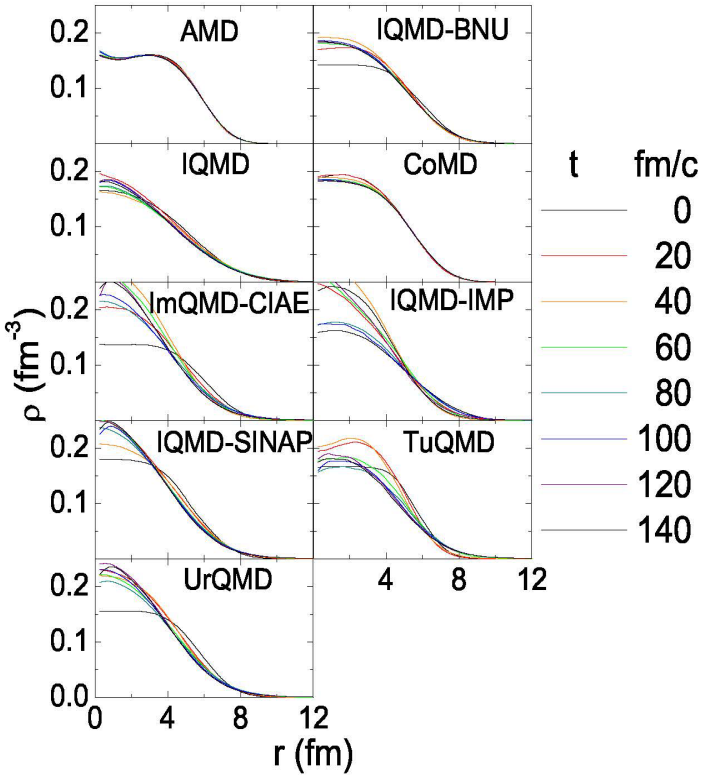

FIG. 3: (Color online) Time evolution of the density distributions in a single Au nucleus in steps of 20 fm/c (see legend for explanation of the different color lines) for QMD-type models at b = 20 fm.

more deterministic nature of the BUU method.

There are also differences in the evolution of the neck between 60 and 100 fm/c. In BUU the neck is usually fatter and stretches out longer (also in AMD). In the breaking of the neck fine structures (or even small fragments) appear. The residues are strongly deformed for a long time. In QMD the neck breaks faster and the residues rather quickly approach a spherical shape. Again these differences are mostly due to the averaging, since in single QMD events fragments are formed in the neck as shown in the right panels of Fig. 6.

There are also differences in the later dynamical evolution of the residues. In BUU one sees in some codes a kind of monopole oscillation (e.g., in pBUU, SMF, but also in AMD), while in QMD the residues show a stronger damping.

Considering these differences it will not be surprising that different codes will show differences in the collision terms discussed in the next subsection, and in observables discussed in subsection C. The anti-symmetrized code AMD shows features which are more similar to the BUU behavior than to the other QMD codes.

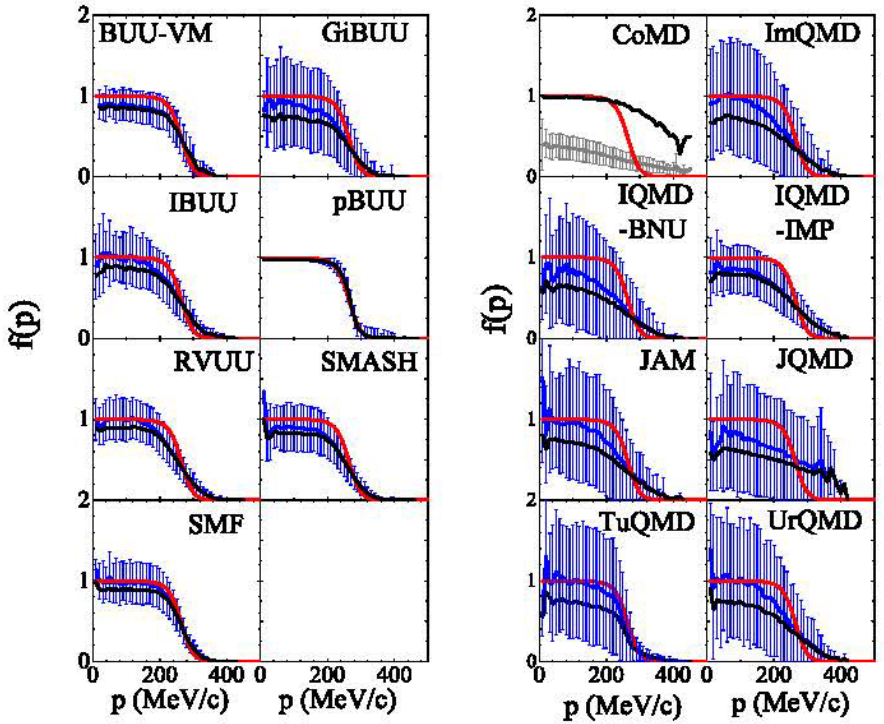

FIG. 7. Distribution of occupation probabilities (blue) in the first time step of the simulation for the $T = 5$ MeV initialization with the mean and variance shown by the blue curve and the blue error bars. Left panels show results for BUU-type codes and right panels for QMD-type codes. The average blocking probabilities are shown as the black curve (see text). The Fermi-Dirac distribution with $T = 5$ MeV used for initialization is represented with the solid line (red). The gray line and error bars for CoMD are explained in the text.

The Microscopic Interaction

Inspired from the Gogny interaction

μ= 1.1 fm

$$V_\mu(\mathbf{r},\mathbf{r'}) = [P_2 + 2P_3(\frac{\rho}{\rho_0})^{\sigma-1}]e^{-(\mathbf{r}-\mathbf{r'})^2/\mu^2}$$

$$V_0(\mathbf{r},\mathbf{r'}) = \frac{1}{\rho_0}[P_{20} + \frac{2P_{30}}{\sigma+1}(\frac{\rho}{\rho_0})^{(\sigma-1)}]\delta(\mathbf{r}-\mathbf{r'})$$

$$V^0_{sy}(\mathbf{r},\mathbf{r'}) = \frac{1}{\rho_0}P_{40}(\frac{\rho}{\rho_0})^{(\gamma-1)}(2\delta_{\tau-\tau'}-1)\delta(\mathbf{r}-\mathbf{r'})$$

$$V^\mu_{sy}(\mathbf{r},\mathbf{r'}) = \frac{1}{\rho_0}P_4(\frac{\rho}{\rho_0})^{(\gamma-1)}(2\delta_{\tau-\tau'}-1)e^{-(\mathbf{r}-\mathbf{r'})^2/\mu^2}]$$

$$V_S(\mathbf{r},\mathbf{r'}) = \frac{1}{\rho_0}P_\pi(\frac{\rho}{\rho_0})^{(\gamma-1)}\delta_{s+s'}\delta_{\tau-\tau'}\delta(\mathbf{r}-\mathbf{r'})$$

MF limit

$$\Phi^i(\mathbf{r}) = \frac{1}{\sqrt{V}}e^{i\mathbf{k}_i\mathbf{r}}$$

$$\Psi^{i,j}(\mathbf{r},\mathbf{r'}) = \Phi^i(\mathbf{r})\Phi^j(\mathbf{r'})$$

Not identical

MD approach

$$\Phi^i(\mathbf{r}) = \frac{1}{(2\pi s^2)^{3/2}}e^{-\frac{(\mathbf{r}-\mathbf{r}_{0,i})^2}{4s^2}+i\mathbf{k}_{0,i}\mathbf{r}}$$

$$\Psi^{i,j}(\mathbf{r},\mathbf{r'}) = \frac{1}{\sqrt{2}}[\Phi^i(\mathbf{r})\Phi^j(\mathbf{r'}) - \Phi^{*,i}(\mathbf{r'})\Phi^{*,j}(\mathbf{r})]$$

Identical

The effective interaction is modelled through the following two conditions on the two-body wave functions

$$\langle\dot{\mathbf{r}}_i\rangle = \frac{\partial H}{\partial\langle\mathbf{p}_i\rangle}, \quad \langle\dot{\mathbf{p}}_i\rangle = -\frac{\partial H}{\partial\langle\mathbf{r}_i\rangle}$$

$$H = \sum_i \frac{\langle\mathbf{p}_i\rangle^2}{2m} + A\frac{3\sigma_p^2}{2m} + V.$$

$\langle\mathbf{r}_i\rangle = \mathbf{r}_{0,i}$ $\quad$ $\langle\mathbf{p}_i\rangle = \hbar\mathbf{k}_{0,i}$

Source of many-body correlations in phase space

MF limit (uniform NM)

$$\Delta E_2^{ex}(\mathbf{k}_1,\mathbf{k}_2) = -\frac{P_2}{V}(\sqrt{\pi}\mu)^3 e^{-\mu^2(\mathbf{k}_1-\mathbf{k}_2)^2/4}$$

$$E_{MF} = \overline{A_{i,j}(r,r')} \times \overline{B_{i,j}(k,k')}$$

a further integration on the single particle states with momenta $\mathbf{k}_1$ and $\mathbf{k}_2$ gives for protons p or neutrons n (q) the following contribution to the potential energy per nucleon :

$$E_2^{q,ex} = -\frac{9}{16}P_2\frac{\pi^{3/2}}{k_F^6}\rho I_q \equiv P_2 R_q(\rho,\beta), \quad (15)$$

$$I_q = \int_o^{k_{Fq}} g(k)k^2dk \quad (16)$$

with

$$g(k) = \frac{2}{\mu k}\left[e^{-\mu^2(k+k_{Fq})^2/4} - e^{-\mu^2(k-k_{Fq})^2/4}\right] + \sqrt{\pi}\{[erf[\mu(k+k_{Fq})/2] + erf[\mu(k-k_{Fq})/2]\} \quad (17)$$

MD approach

In quantum molecular dynamics approaches single particles wave functions are represented through wave packets with fixed width (s=1.15 fm in CoMD).

$$\Phi^i(\mathbf{r}) = \frac{1}{(2\pi s^2)^{3/2}} e^{-\frac{(\mathbf{r}-\mathbf{r}_{0,i})^2}{4s^2} + i\mathbf{k}_{0,i}\mathbf{r}} \quad (14)$$

For identical particles, using the anti-symmetrized 2-body wave-packet function, we obtain the 2-body exchange contribution to the energy for the generic couple as follows:

$$E_2^{1,2,ex} \equiv \frac{1}{2}P_2 R^{1,2,ex} \quad (15)$$

$$R^{1,2,ex} = -\frac{1}{8s^3}\xi^3 \times e^{-\frac{1}{4}[\frac{(\mathbf{r}_{0,1}-\mathbf{r}_{0,2})^2}{s^2} + \xi^2(\mathbf{k}_{0,1}-\mathbf{k}_{0,2})^2]}(\delta_{\tau_1-\tau_2}\delta_{s_1-s_2}) \quad (16)$$

with $\xi = \frac{2s\mu}{\sqrt{4s^2+\mu^2}} \equiv \frac{2s\mu}{\alpha}$. τ_i and s_i indicate the nucleon third components of the iso-spin and spin quantum numbers respectively. The total direct term will be:

$$E = \overline{A_{i,j}(r,r')B_{i,j}(k,k')} \neq \overline{A_{i,j}(r,r')} \times \overline{B_{i,j}(k,k')} = E_{MF} + \delta E$$

$$\delta E = \overline{\delta A(r,r')\delta B(k,k')} \neq 0$$

Correlated “fluctuations”

plus correlations generates through the Pauli Constraint

NM at zero Temperature as a reference

E_b=-16 MeV/A

P_0=0.165 fm^{-3}

K_{nm}=240 MeV

E_{sym}=30 MeV

M^*/M=0.67

$(M^*n-M^*p)/M$=0.4β

$E_\pi(\rho_0)$=2 MeV/A (finite system)

L=50-110 MeV

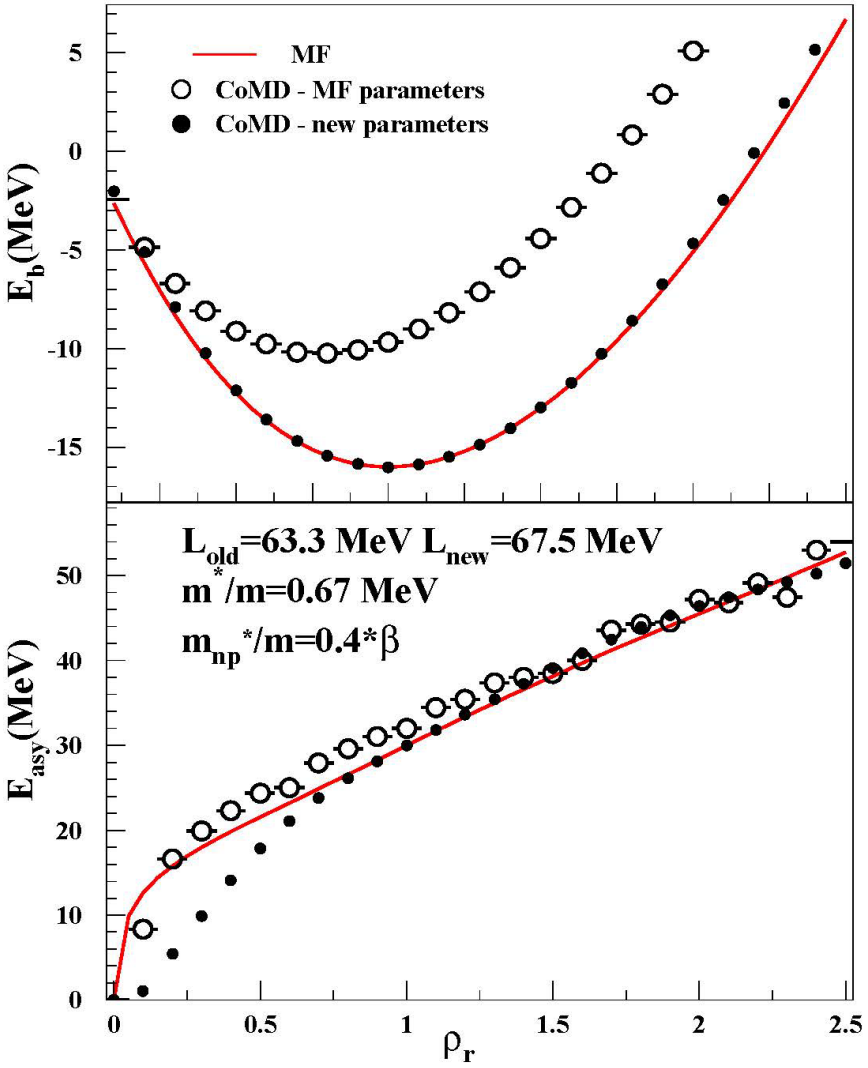

$F_p=F_{calc}-1$

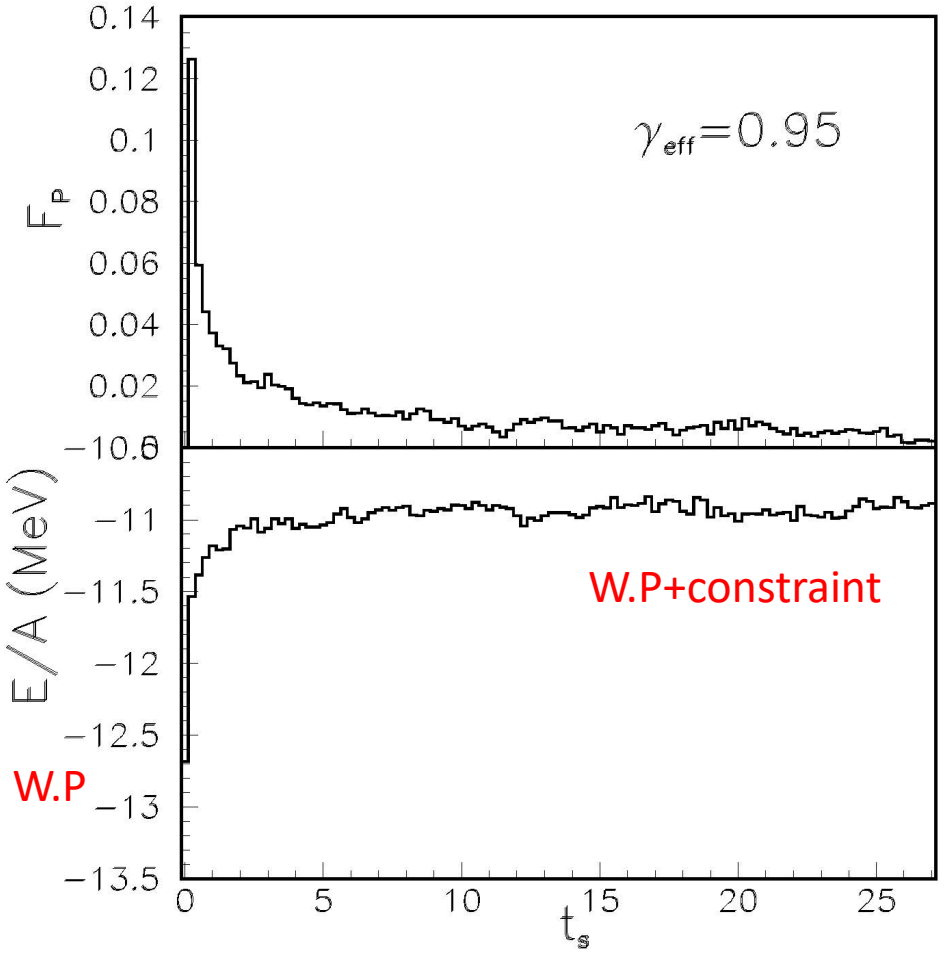

dE_{wp}~3.5 MeV/A

dE_c~2.5 MeV

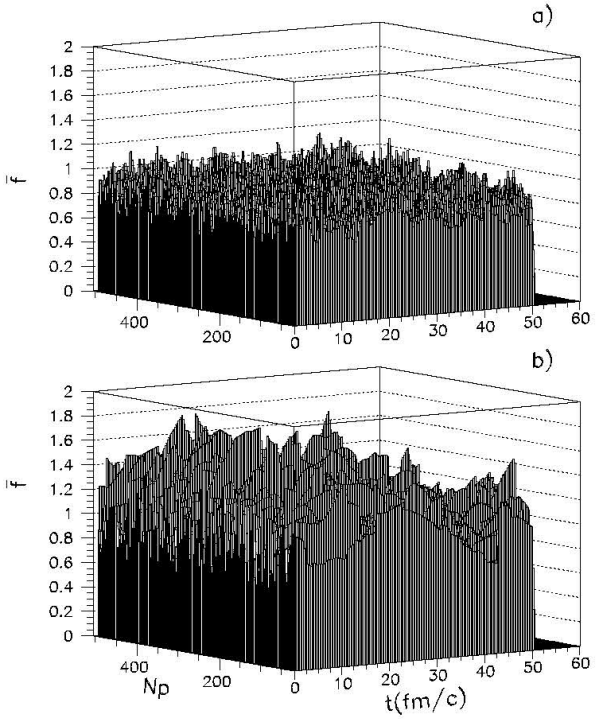

Figure 8: panel a): An an example, by using the interaction parameters shown on the second row of Table 1 we plot the time dependence of the phase-space occupation $\overline{f}$ for each particle (500 neutrons) at the saturation density. panel b): same like panel a) but without the constraint

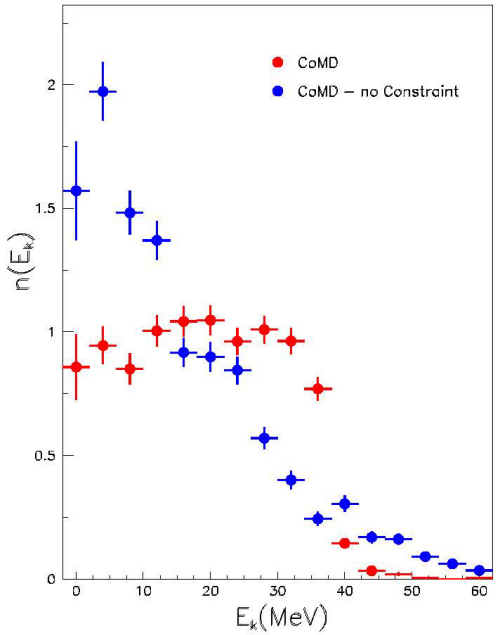

Figure 9: Occupation number as function of the kinetic energy for CoMD c t=50 fm/c a with and without the constraint.

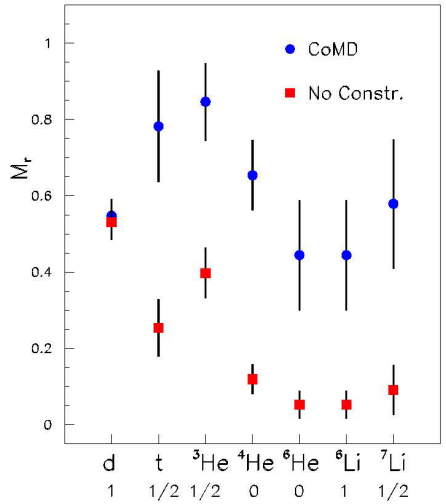

Figure 10: For CoMD and no-constraints at $\rho = 0.2\rho_0$ with different markers the relative produced yields M_r are shown. For each isotope, whose chemical symbol is reported along the horizontal axes, M_r represents the ratio between the yield of isotope having the right spin and the related total yield. The value of the right spin is reported under each chemical symbol. (color on-line)

Submitted for Publication

Many-body correlations and the Iso-vectorial interactions

$$p = 1 \pm k_0 v(r) \quad v(0) = 1 \quad k_0 \geqslant 0.$$

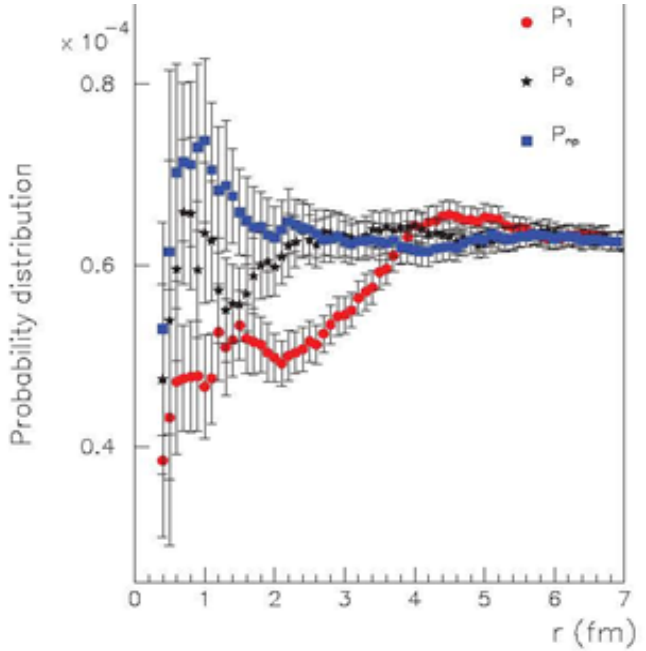

FIG. 2. (Color online) Probability distribution P_1 to find two identical nucleons at a relative distance r. In the same figure P_0 represents the probability evaluated for neutron and proton couples with opposite spin. Finally, P_{np} indicates the probability obtained for neutron-proton couples.

$$\tilde{\rho} = \frac{N^2\widetilde{\rho^{nn}} + Z^2\widetilde{\rho^{pp}}}{N^2 + Z^2},$$
$$\alpha = \frac{\widetilde{\rho^{np}} - \widetilde{\rho}}{\widetilde{\rho}},$$

$$W^C_{\rm isv} = \frac{T_4}{2\rho_0} A^2 \tilde{\rho}\left[\left(1+\frac{\alpha}{2}\right)\beta^2 - \frac{\alpha}{2}\right],$$
$$E^C_{\rm isv} = \frac{T_4}{2\rho_0} F_k^l(\overline{S_v})\tilde{\rho}_A\left[\left(1+\frac{\alpha}{2}\right)\beta^2 - \frac{\alpha}{2}\right],$$
$$E_{\rm bias} = -\frac{T_4}{4\rho_0} F_k^l(\overline{S_v})\tilde{\rho}_A\alpha,$$

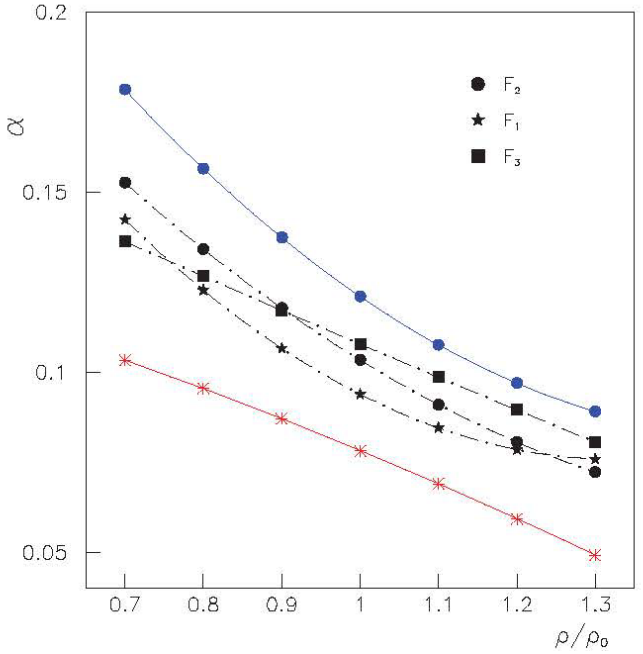

Table 1: For the three investigated cases we report the parameters values characterizing the adopted effective interaction (see the text). The units of the P parameters are MeV. All the cases corresponds to m_r^* and $m_{nr}^* - m_{pr}^*$ equal to 0.67 and 0.42β

P_2	P_3	P_{20}	P_{30}	P_π	P_{40}	P_4	L	σ	γ
1042.8	-434.1	-870.0	169.9	-213.4	478.1	-300.0	63.3	0.9	0.7
368.3	55.9	-490.0	0.82	-198.9	289.4	-150.0	50.6	1.4	0.5
601.7	-19.1	-860.0	187.3	-212.7	477.8	-300.0	81.3	1.2	0,8

Table 2: In the table we report the set of new parameters values P' as obtained from the fit procedure. The global uncertainty on the parameters values as due to the model calculations and fit procedure is of the order of $\pm 2\%$. The error bars represent the statistical uncertainties.

P_2'	P_3'	P_{20}'	P_{30}'	P_π'	P_{40}'	P_4'	L	σ	γ
1776.8	-1302.6	-1503.1	920.8	-171.4	551.1	-425.6	67.5	0.9	0.7
450.8	-82.	-639.0	190.3	-175.7	313.5	-213.1	55.0	1.4	0.5
660.8	-284.7	-1069.7	602.3	-220.3	684.8	-420.6	105.0	1.2	0.8

Finite Systems ^{64,58}Ni+^{48}Ca at different energies.
Comparison between the cases μ=0 and μ= 1.1 fm

Different interactions producing very similar EOS

It is necessary to add this a surface term

$$E_s^i = c_s \nabla^2 S(\mathbf{r}_i)$$

CoMD calculations (No Gemini)

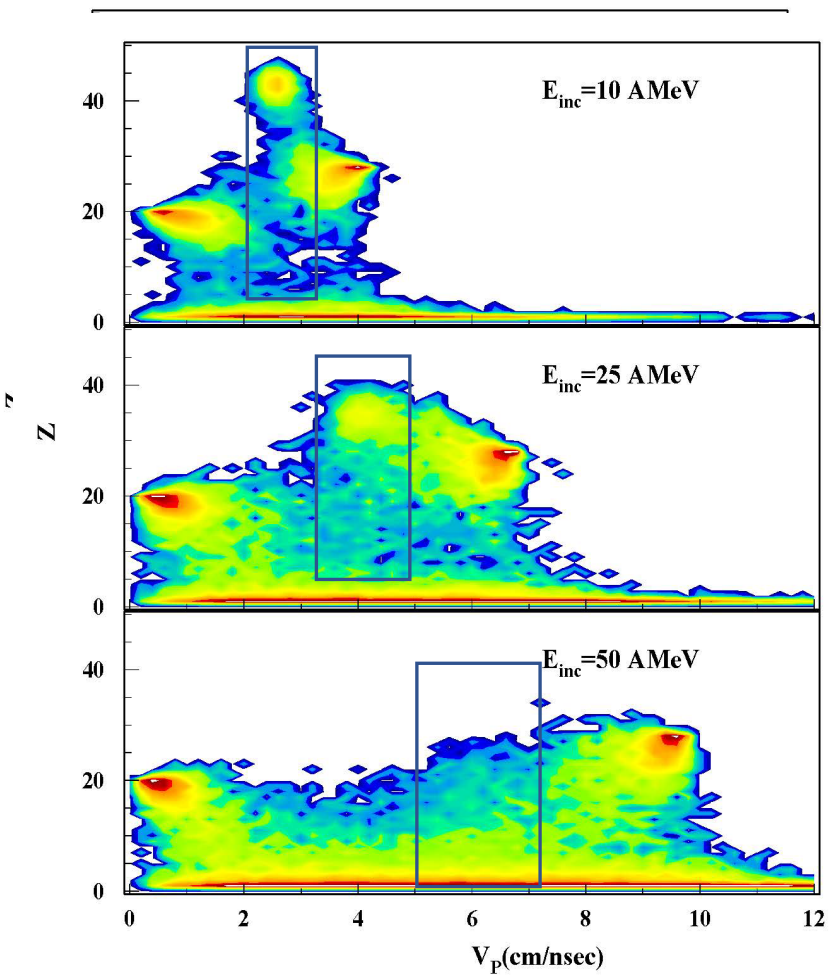

^{64}Ni+^{48}Ca Reaction Mechanisms b=0-5. fm

ICF, IMF production, Fission around the C.M. velocity

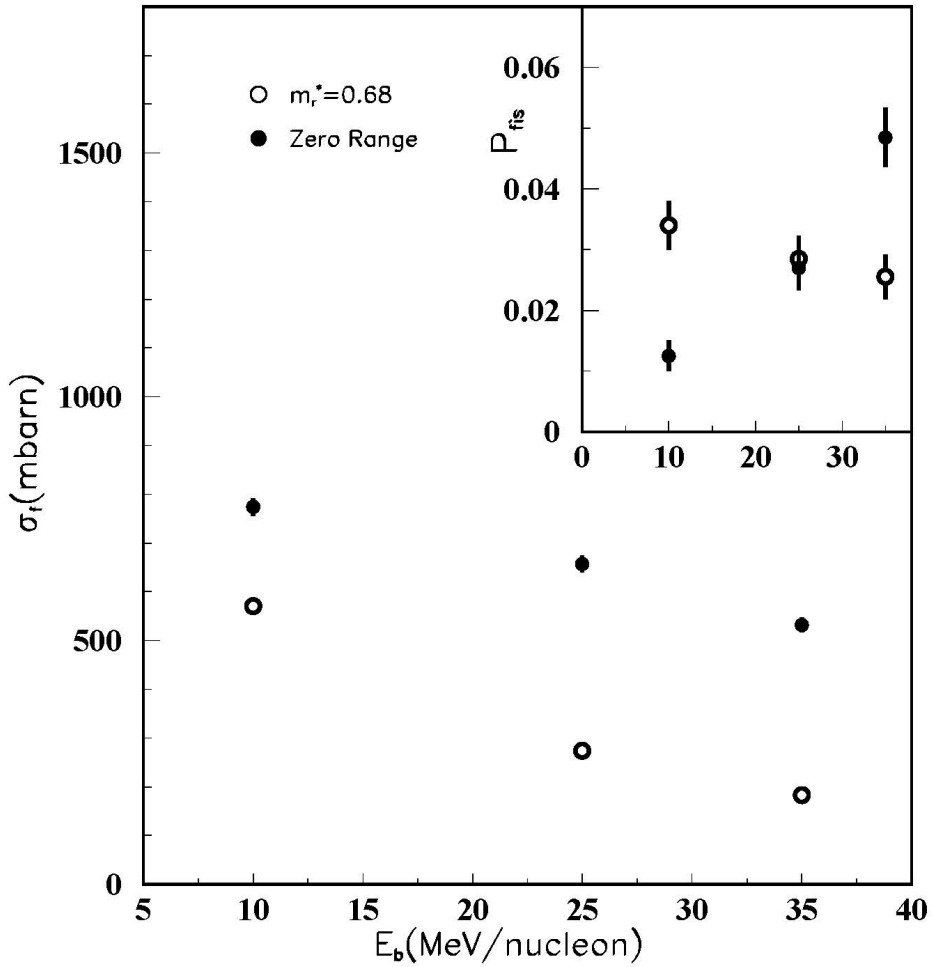

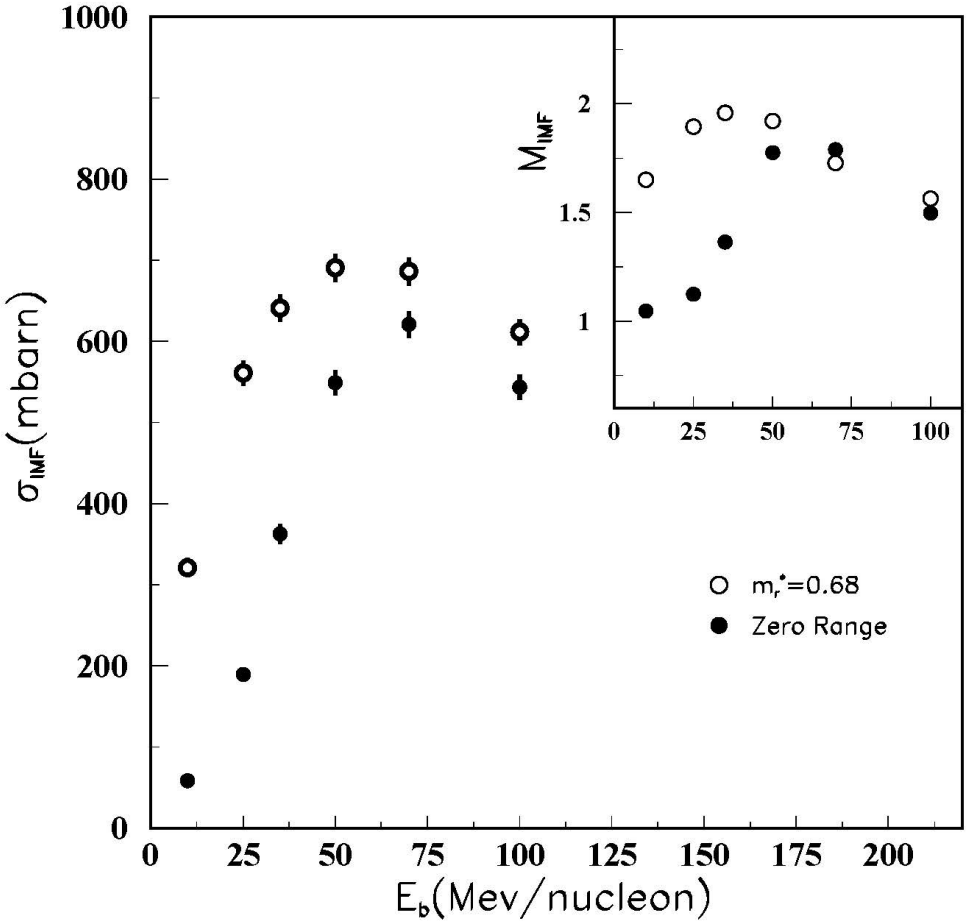

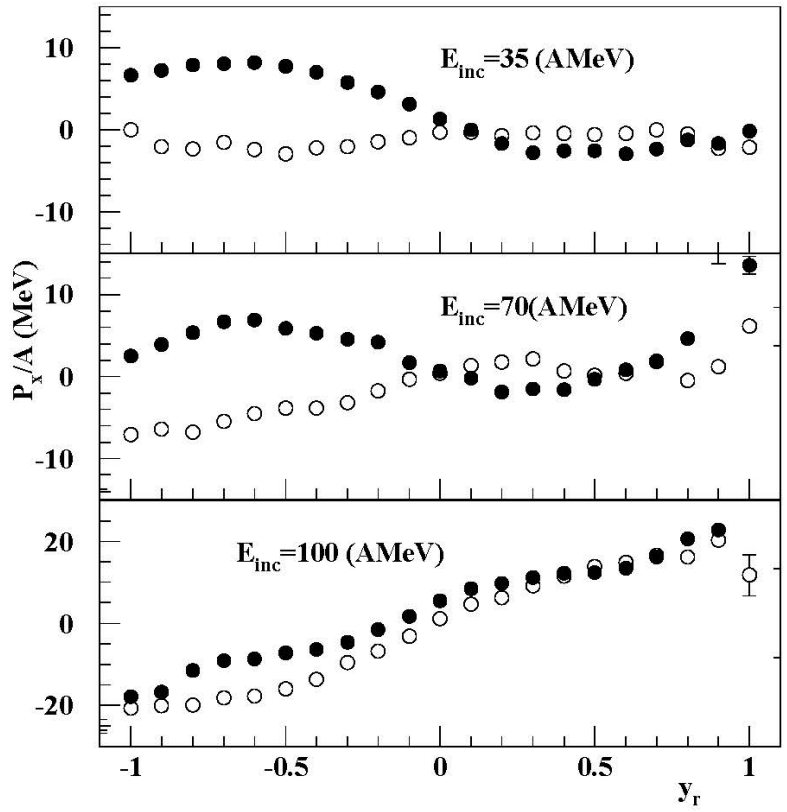

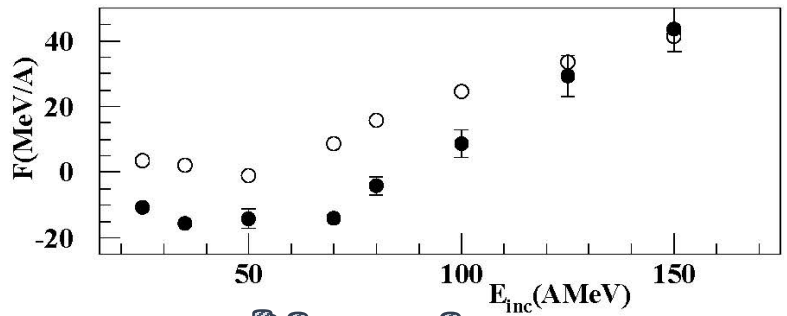

Preliminary

Final Remarks

- In the molecular dynamics model CoMD the strength parameters r elated to the momentum-dependent effective interaction have been revalued to take in to account specific phase-space correlations that are absent in semiclassical mean field approaches.

- ICF, Fission IMF production around the c.m.velocity, flow angles In the energy range 25-100 AMeV are strongly affected by the range of the effective interaction (M*) .

- Around 125-150 MeV these differences are smaller.

- Large differences are still present in others regions of velocities

The Dipolar signal and the Isospin Equilibration Phenomenon

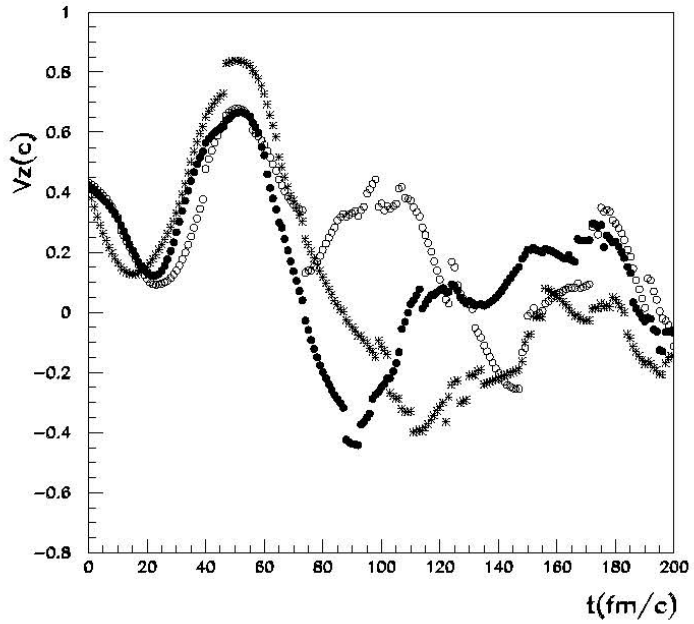

FIG. 1. Time derivative of the total dipole along the beam directions as function of time calculated by means of the CoMD model. The three different symbols are related to three different microscopic realizations of the ^{40}Ca+^{48}Ca system at 25 MeV/nucleon and for an impact parameter $b=0$ fm.

$$\langle \vec{D} \rangle = \left\langle \sum_{i=1}^{m} Z_i (\vec{V}_i - \vec{V}_{c.m.}) \right\rangle_{\mathcal{K}} .$$

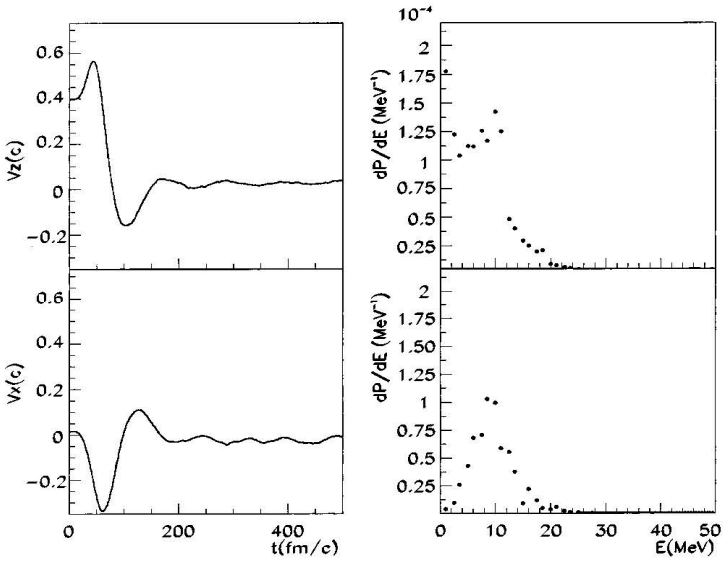

FIG. 6. On the right side are shown the time derivative of the average total dipole along the beam direction V_Z and along the impact-parameter direction V_X as function of time, for the ^{40}Ca $+^{48}$Ca system at 25 MeV/nucleon and $b=3.5$ fm. On the left side are shown the related γ-ray yield distributions. The uncertainties on the y-axis related to the ensemble averages are of the order of 2%. The energy axis of every point is undetermined within ± 650 keV.

In binary systems, for example, in the absence of dynamical neutron-proton collective motion, we have $\langle \vec{D} \rangle \equiv \vec{D}_m = \frac{1}{2}\langle \mu \rangle (\langle \beta_2 \rangle - \langle \beta_1 \rangle)(\langle \vec{V}_1 - \vec{V}_2 \rangle)$. Here, μ is the reduced mass number of the system, β_1 and β_2 are the isospin asymmetries of the two partners 1 and 2, and finally $\vec{V}_1$ and $\vec{V}_2$ are the related velocities. In the above expression, we have assumed

In particular, these expressions were determined in a phe-
omenological way from the GDR ground-states properties.
ccording to Ref. [16], they remain valid at finite temperature.

APPENDIX B

In this Appendix we want to clarify the definition and
roperties of the ensemble average of the first time derivative
f the total dipole $\vec{V}$ expressed through Eqs. (8)–(10). This
mple derivation can be useful since it naturally produces an
xplicit definition of the correlation functions introduced in
q. (9) in terms of an event-by-event analysis performed on
ie experimental data.

In the following, we will describe the multiparticle event
very long time when all the fragments are cold. In this
mit and for our aims, the disassembly of the system can be
escribed through the velocities $\vec{v}_i^k$, the charges Z_i^k, or the mean
omentum $\langle \vec{P}^k_{Z,A} \rangle$ and the multiplicity $m^k_{Z,A}$ of the particle i
aving charge Z and mass A in the generic event k. Therefore,
e can write the following set of identities:

$$\vec{V}^k(t \to \infty) = \sum_{i=1}^{M^k} Z_i^k \vec{v}_i^k = \sum_{Z,A} \frac{Z}{A} m^k_{Z,A} \langle \vec{P} \rangle^k_{Z,A}, \tag{B1}$$

$$\sum_{Z,A} m^k_{Z,A} = M^k, \tag{B2}$$

$$\langle \vec{P} \rangle^k_{Z,A} = \frac{\sum_{l=1}^{m^k_{Z,A}} \vec{P}_l^k}{m^k_{Z,A}}, \tag{B3}$$

here the index l varies over all the particles having the same
ass A and charge Z in the event k.

By performing the ensemble average on N events, we obtain

$$\overline{\vec{V}(t \to \infty)} = \sum_{Z,A,k=1}^{N} \frac{Z}{A} \frac{m^k_{Z,A} \langle \vec{P} \rangle^k_{Z,A}}{N} = \sum_{Z,A,k=1}^{N} \frac{Z}{A} \overline{m_{Z,A}} \, \overline{\langle \vec{P} \rangle_{Z,A}} \, C^{Z,A}_{\langle \vec{P} \rangle}, \tag{B4}$$

$$C^{Z,A}_{\langle \vec{P} \rangle} \equiv \frac{\overline{m_{Z,A} \langle \vec{P} \rangle_{Z,A}}}{\overline{m_{Z,A}} \, \overline{\langle \vec{P} \rangle_{Z,A}}} = N \frac{\sum_{k=1}^{N} m^k_{Z,A} \langle \vec{P} \rangle^k_{Z,A}}{\left(\sum_{k=1}^{N} m^k_{Z,A} \right) \left(\sum_{k=1}^{N} \langle \vec{P} \rangle^k_{Z,A} \right)}. \tag{B5}$$

hese equations clarify the meaning of Eqs. (8) and (9).

To prove the validity of Eq. (10) we now consider a shorter
me t and we suppose that the produced fragments are now
xcited. Consequently, the expression of $\vec{V}^k$ for the event k can
e written as

$$\vec{V}^k(t) = \sum_{i=1}^{M'^k} Z_i'^k \vec{v}_i'^k + \sum_{i=1}^{m^k} \vec{S}_i. \tag{B6}$$

The primed symbols represent the different quantities evaluated at time t. $\vec{S}_i$ stands for possible dipolar intrinsic excitations of the complex fragments that are produced with a multiplicity m^k. We can now suppose for simplicity and without losing generality that the chosen time t is such that

$$Z_i'^k = Z_i^k, \quad i = 1, \quad M'^k - 1 \tag{B7}$$

$$\vec{v}_i'^k = \vec{v}_i^k, \quad i = 1, \quad M'^k - 1 \tag{B8}$$

$$M'^k = M^k - 1. \tag{B9}$$

We can also suppose that the last fragment M'^k will subsequently decay into the fragments labeled with indexes $M^k - 1$, and M^k observed at longer time [see Eqs. (B1)–(B3)]. Therefore

$$Z'^k_{M'^k} = Z^k_{M^k-1} + Z^k_{M^k}, \tag{B10}$$

$$\vec{v}^k_{M^k-1} = \vec{v}'^k_{M'^k} + \vec{v}_r^{M^k-1}, \tag{B11}$$

$$\vec{v}^k_{M^k} = \vec{v}'^k_{M'^k} + \vec{v}_r^{M^k}, \tag{B12}$$

$$\vec{V}^k(t \to \infty) = \vec{V}^k(t) + Z^k_{M^k-1} \vec{v}_r^{M^k-1} + Z^k_{M^k} \vec{v}_r^{M^k} + \sum_{i=1}^{m^k} \vec{S}_i, \tag{B13}$$

where $\vec{v}_r^{M^k-1}$ and $\vec{v}_r^{M^k}$ are the relative velocities of the particles $M^k - 1$ and M^k with respect to the common c.m. velocity $v'^k_{M'^k}$. In the following, for simplicity, we perform an ensemble average on all the events having this structure. In other words, we perform an ensemble average on the process leading to the particle decay of the fragment M'^k. The results obtained with this average obviously will remain valid for a more extended average, which includes events having different structures:

$$\overline{\vec{V}^k(t \to \infty)} = \overline{\vec{V}^k(t)} + \overline{Z^k_{M^k-1}} \, \overline{\vec{V}_r^{M^k-1}} C_{M^k-1} + \overline{Z^k_{M^k}} \, \overline{\vec{V}_r^{M^k}} C_{M^k} + \sum_{i=1}^{m^k} \overline{\vec{S}_i} \tag{B14}$$

where C_{M^k-1} and C_{M^k} are the correlation functions between charges and the relative velocities of the fragments generated through the decay of the source labeled with M'^k. We now assume that $t > t_{\rm eq}$; $t_{\rm eq}$ is a time after which one can consider statistical excitation of the dipolar mode and particles emission according to the compound nucleus mechanism. Under this condition, we get

$$\overline{\vec{S}_i} = 0 \qquad i = 1, m^k, \tag{B15}$$

$$\overline{\vec{V}_r^{M^k-1}} = \overline{\vec{V}_r^{M^k}} = 0. \tag{B16}$$

The first equation reflects the definition itself of dipolar statistical excitations (see also Ref. [22]). In fact, in this case the dipolar signals correspond to the fluctuations around the ensemble averages. The ensemble averages of these signals are zero by definition. The second equation reflects the results of the isotropic emission that characterizes the particle decay from a hot compound nucleus. Therefore, we finally obtain

$$\overline{\vec{V}^k(t \to \infty)} = \overline{\vec{V}^k(t > t_{eq})}, \tag{B17}$$

which is just Eq. (10) of the text.

Pre-Equilibrium ɣ-ray Emission and Isospin Dynamics

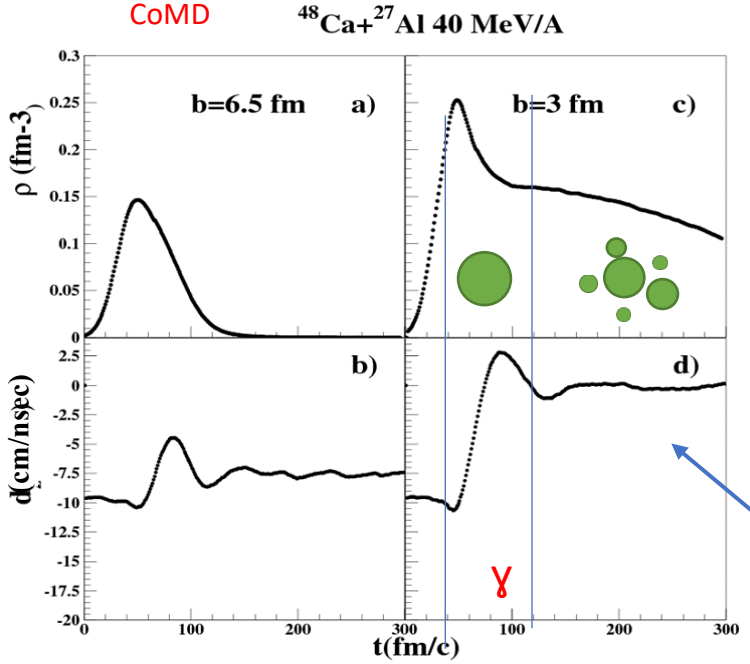

Asymptotic Dipolar signal

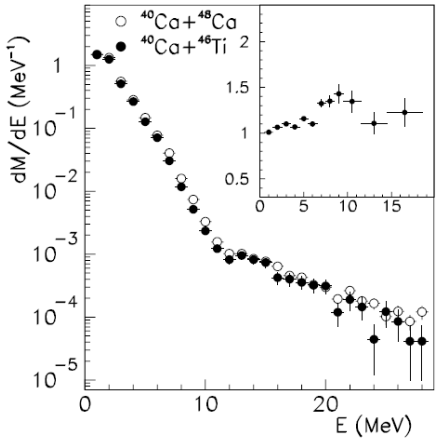

- Pre -Equilibrium ɣ- ray emssion was already investigated as the result of the excitation of a «special» collective mode in semi-inclusive measurements
- Further investigations established a direct connection between this emission and the dynamics (beyond statistical decays) of the processes leading to the equilibration of the charge / mass ratio in phase-space after the collision – > connection with EoS, iso-vectorial forces (Esym) at different densities.

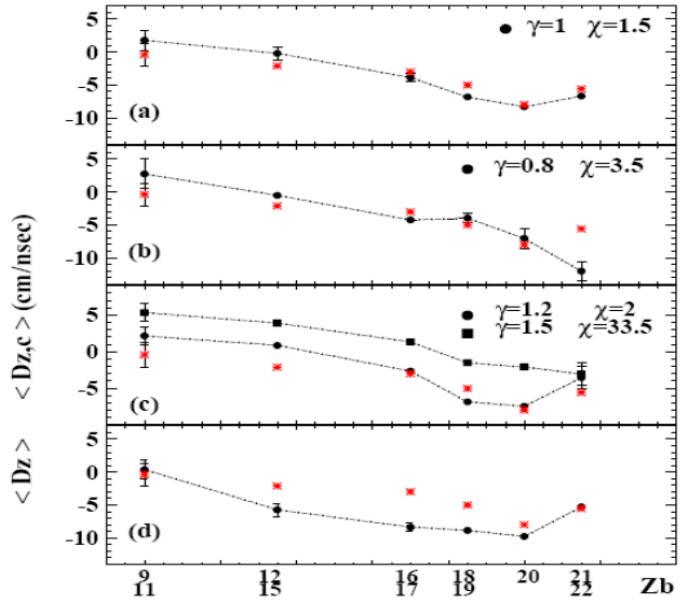

L =87.6±14 MeV
S(ρ_0)=32 MeV

- We started to study this process through the measurement of the average Dipolar signal obtained from the identified fragments in rather well reconstructed events. (CHIMERA – rather selective conditions)
- The observation of the pre-equilibrium radiation (CsI CHIMERA sphere) in coincidence with well reconstructed multi-break-up events could unequivocally fix, through the associated spectral characteristics, the time intervals of the processes -> density and / or density intervals explored <- > **Forces** -> Stable beam (also and especially neutron rich) 4-6 times more intense

M.Papa et al; Phys ReV C 91, 041609 (2015) ;J. Phys Conf. Ser 1643 012103 (2020);

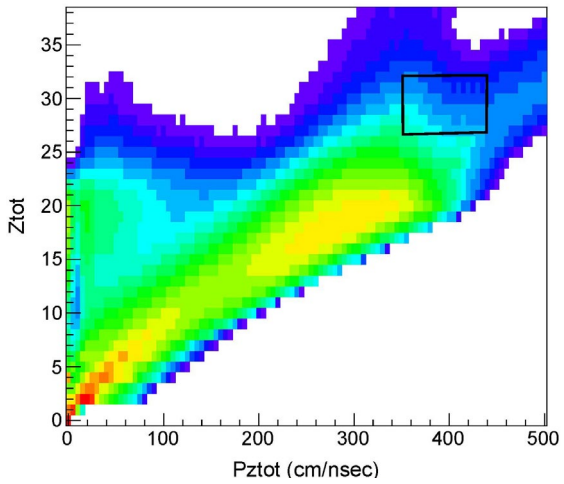

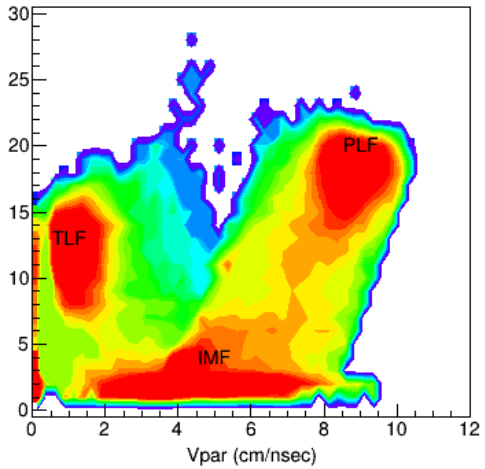

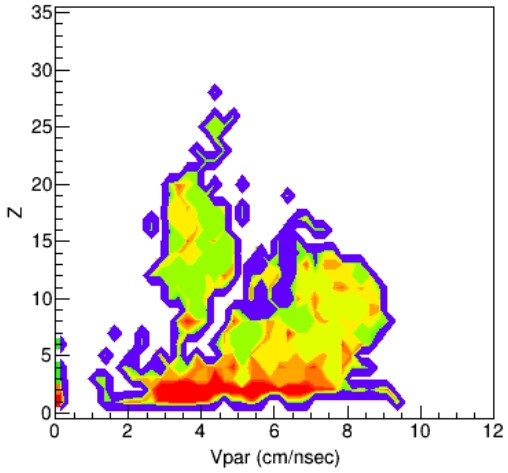

NEWCHIM/ CHIRONE at LNS

G.Cardella,
P.Russoto,
C.Maiolino
E.Geraci
.....

Perspectives

--To complete the investigation on the effects produced by the many-body correlations (at the semi-classical level) on EDFs. To understand how this correlations affect observables usually studied in Heavy-Ion Collision.

-- Extend these studies to low densities to include cluster formation processes

-- Progress in the studies on the Isospin-Equilibration phenomenon through the study of the dipolar signal (Equil2 experiment) for different degrees of centrality,, (IMF production, hot sources disassembly) – comparison with model calculations.